Surface Science 192 (1987) 47–65
North-Holland, Amsterdam

ADSORPTION OF HCOOH ON Rh(111) AND ITS REACTION WITH PREADSORBED OXYGEN

Frigyes SOLYMOSI, János KISS and Imre KOVÁCS

Reaction Kinetics Research Group of the Hungarian Academy of Sciences and Institute of Solid State and Radiochemistry, University of Szeged, P.O. Box 105, H-6701 Szeged, Hungary

Received 25 March 1987; accepted for publication 30 July 1987

The interaction of formic acid with clean and oxygen-dosed Rh(111) surfaces has been investigated by electron energy loss (in the electronic range), thermal desorption and photoelectron spectroscopy. Formic acid adsorbs readily on the Rh(111) surface at 100 K with a high sticking probability. Three adsorbed states have been distinguished: a condensed layer ($T_p = 170$ K), a chemisorbed layer ($T_p = 202$ K) and the formation of formate species. The latter is stable up to 200 K, but decomposes completely at 200–250 K. The major products are: H_2 ($T_p = 323$ K) and CO_2 ($T_p = 255$–290 K), but H_2O ($T_p = 263$ K) and CO ($T_p = 530$ K) are also formed. Preadsorbed oxygen exerted a readily observable influence on the interaction of HCOOH with the Rh(111) surface. It increased the extent of dissociation of HCOOH and extended the region of stability of surface formate by at least 80–100 K. This was demonstrated by higher stability of photoemission peaks due to formate and by simultaneous production of CO_2 and H_2O with $T_p = 377$–385 K at saturation oxygen coverage.

1. Introduction

It has emerged that adsorbed formate is one of the surface intermediates in various catalytic reactions on supported Rh catalysts. It has been detected by infrared spectroscopy in the water–gas shift reaction [1], in the synthesis and decomposition of CH_3OH [2], and in the methanation of CO [3,4] and CO_2 [5–7]. Strong bands due to adsorbed formate are also produced in the low-temperature surface interaction of $H_2 + CO_2$ [8–10]. The situation is complicated by the fact that the formate species detected is mostly located not on the metal, but on the support. However, we recently showed that even the formate residing on the support can be transformed into CH_4 by reaction with hydrogen activated on the Rh. Although this route was considered to be a minor one in the production of CH_4, it was demonstrated that formate species bonded adjacent to the Rh cannot be regarded as a totally inactive surface species in the hydrogenation of CO and CO_2 [11]. An important contribution to this field was provided by Deluzarche et al. [12–14], who developed a sensitive method of chemical trapping for the detection of surface formate.

They presented convincing evidence that the formate species is an important surface intermediate in CH_3OH synthesis. More information on the role of the formate species in the reactions of carbon oxides with H_2 on other catalysts can be found in an excellent review by Deluzarche et al. [14].

In order to clarify the role of the formate species in the above reactions, we need to know more about its surface behavior and reactions on the clean metals themselves. We earlier investigated the adsorption of HCOOH on polycrystalline Rh [15]. In the present work the interaction of HCOOH with an ordered surface structure of Rh, i.e. the (111) face is examined, in combination with a study of the effect of preadsorbed oxygen. In a following paper [16], we shall report on the effect of potassium additive on the adsorption and decomposition of HCOOH on the Rh(111) surface.

2. Experimental

Experiments were performed in a stainless steel UHV chamber equipped with several gas inlets, a four-grid retarding field analyser for Auger electron spectroscopy and for low-energy electron diffraction (LEED) and a quadrupole mass analyser for thermal desorption spectroscopy. The electron energy loss spectra (EELS in electronic range) were taken by means of cylindrical mirror analyzer. Changes in work function were obtained from the low energy cut off in the EEL spectra [17]. The beam energy was 70 eV, the beam intensity was restricted to 0.05 μA. The vacuum system was evacuated with ion pumps and a titanium getter pump.

UPS measurements were performed in an other UHV system. The photoelectrons were detected by an electrostatic hemispherical energy analyzer (Leybold-Hereaus LHS 10). The photon source (He I, He II) was pumped differentialy. The UPS spectra were taken with an instrumental resolution of 0.2 eV. All binding energies are referenced to the Fermi level of rhodium. The difference spectra were obtained by means of a Tracor TN 1710 multichannel analyzer. The spectra were stored by a microcomputer connected to the Tracor analyzer. The vacuum system was evacuated by a turbomolecular pump and a titanium getter.

The Rh crystal was cut from a single crystal. It was a product of Materials Research Corporation; the purity was 99.99%. The sample was heated resistively and its temperature was measured by a chromel–alumel thermocouple spot-welded to the edge of crystal. For low-temperature measurements the Rh sample was cooled by a Ta foil spotwelded to the sample and connected to a liquid-nitrogen-cooled stainless tube. As the Rh sample has been used in a number of our previous studies, it was sufficient to clean the sample by argon ion bombardment (600 eV, 1×10^{-6} Torr Ar, 3 μA for 10–30 min), and annealing at 1270 K for some minutes.

HCOOH was a product of Merck. It was purified in the manner reported earlier [15]. Extended vacuum evaporation removed CH_3OH and CH_3COOH.

3. Results

3.1. Clean Rh(111)

3.1.1. Thermal desorption measurements

Fig. 1 shows some characteristic desorption spectra of HCOOH as a function of HCOOH exposure at 100 K. Low exposure produced only a single peak (β) with a peak temperature, $T_p = 202$ K, which did not exhibit a dependence on the HCOOH exposure. Below ~ 0.5 L HCOOH exposure, no desorption of HCOOH was detected. Above a HCOOH exposure of 5 L another peak (α) developed, with a T_p of 170 K, which slightly increased with coverage indicating a zero-order kinetics. While the β-state became saturated at about 6 L, saturation was not reached for the α-peak up to 30 L (fig. 1).

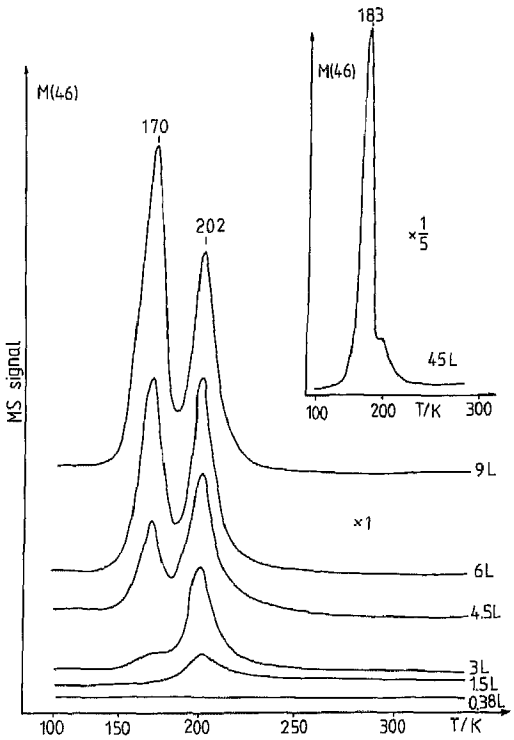

Fig. 1. Thermal desorption spectra of HCOOH following HCOOH adsorption on clean Rh(111) at 100 K.

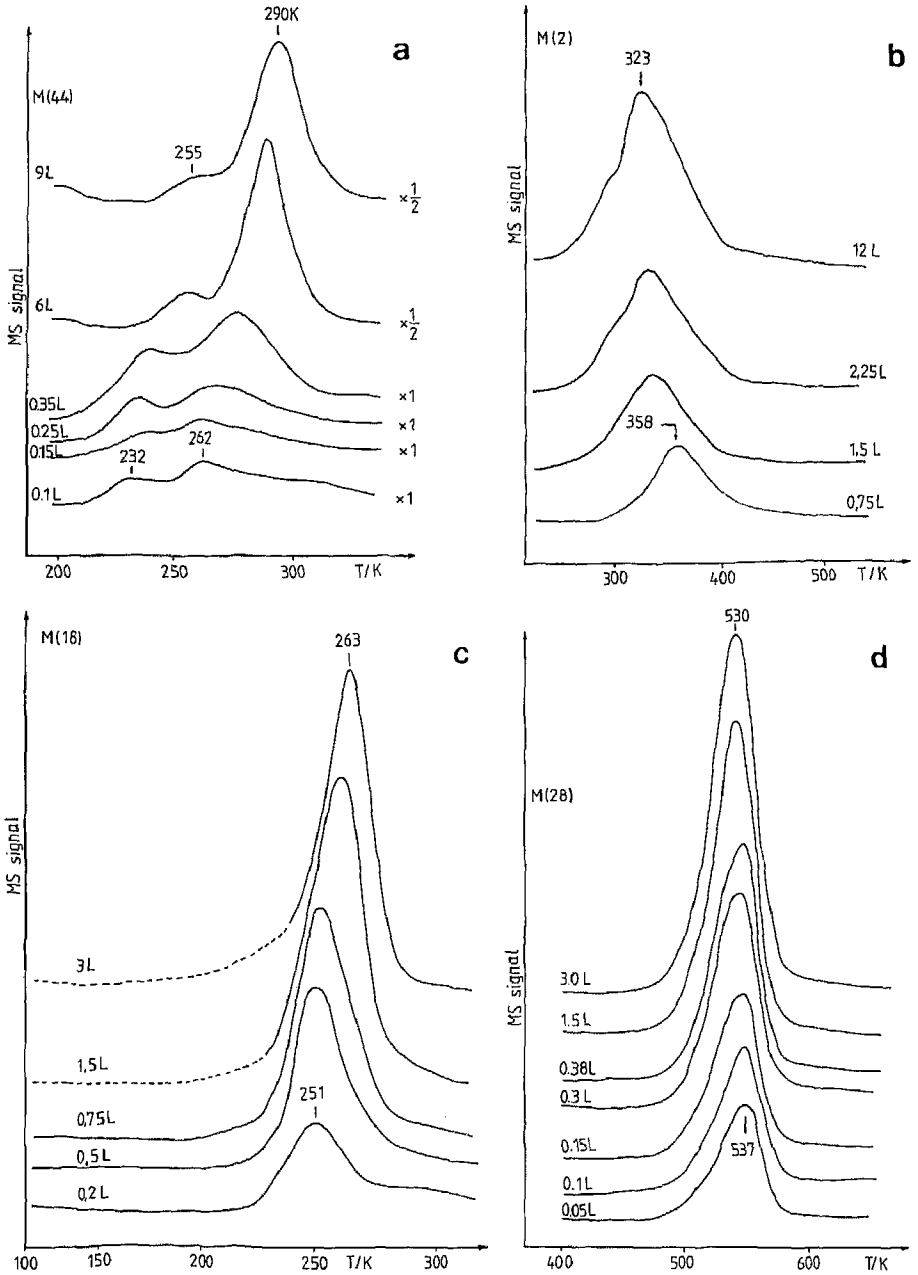

Fig. 2. Thermal desorption of CO_2 (a), H_2 (b), H_2O (c) and CO (d) following HCOOH adsorption on clean Rh(111) at 100 K.

Quantitative analysis of the peak areas, taking into account the pumping rate and mass spectrometer sensitivity for HCOOH, demonstrated that in the β-state the surface concentration was approximately 5.5×10^{13} HCOOH molecules/cm^2. As regards the accuracy of this value, we may recall the statement of Christmann and Demuth [18]: "Such absolute values are inherently uncertain ($\pm 50\%$) as the effective pumping speed and gauge calibration factors are not precisely defined".

Besides HCOOH, the formation of CO_2, H_2, H_2O and CO was observed at higher temperatures, suggesting that a more strongly adsorbed species remained on the surface and decomposed to these products at higher temperatures. Even at the lowest exposures CO_2 desorbed in two peaks, with $T_p = 232$ K (β_1) and 262 K (β_2). With increase of the HCOOH exposure, the peak temperatures of both peaks shifted to higher values, 255 K (β_1) and 290 K (β_2) (fig. 2a). An important feature is that the amount of CO_2 desorbed in the β_2 state increased considerably with rise of the HCOOH exposure: the corresponding increase was much less for the β_1 state. In contrast to the behavior of CO_2, the H_2 desorption maximum shifted from 358 to 323 K with increasing HCOOH exposure. At higher exposures, a shoulder developed at 293 K (fig. 2b). A small amount of H_2O was also detected among the desorption products: a desorption maximum was located at 251–263 K (fig. 2c). The desorption of CO occurred at highest temperatures, with a slight shift in its T_p from 537 to 530 K (fig. 2d).

In fig. 3 the amounts of the desorption products are plotted as a function of the HCOOH exposure. It appears that saturation for H_2 and CO_2 is attained at about 10–12 L, for H_2O and CO at lower exposure at 2–3 L. The ratio H_2/CO_2 is approximately 1.0 at all coverages. Whereas the ratio CO_2/CO is below 1 at the lowest HCOOH exposure, it increases to about 4 at saturation, indicating a change in the stoichiometry of surface decomposition. Taking into account the sum of CO and CO_2 at saturation and assuming that they are formed in the decomposition of adsorbed formate species (see later), we find that the concentration of the strongly adsorbed formate species is 6.3×10^{14} HCOO molecules/cm^2.

The initial sticking coefficient (S_0) of HCOOH adsorption, calculated from the plot of the total amount of chemisorbed HCOOH against exposure, was found to be ~ 1.

3.1.2. EELS measurements

The characteristic of the EEL spectrum of the Rh(111) sample agreed well with those established previously for a clean Rh surface, which have been discussed in detail [19,20]. The adsorption of HCOOH on a clean Rh(111) surface produced a new loss at 11.3 eV at 100 K and at low exposure (0.3 L). Its intensity increased with the HCOOH exposure, and from about 2 L new loss features appeared at 14.8 and 7.9 eV.

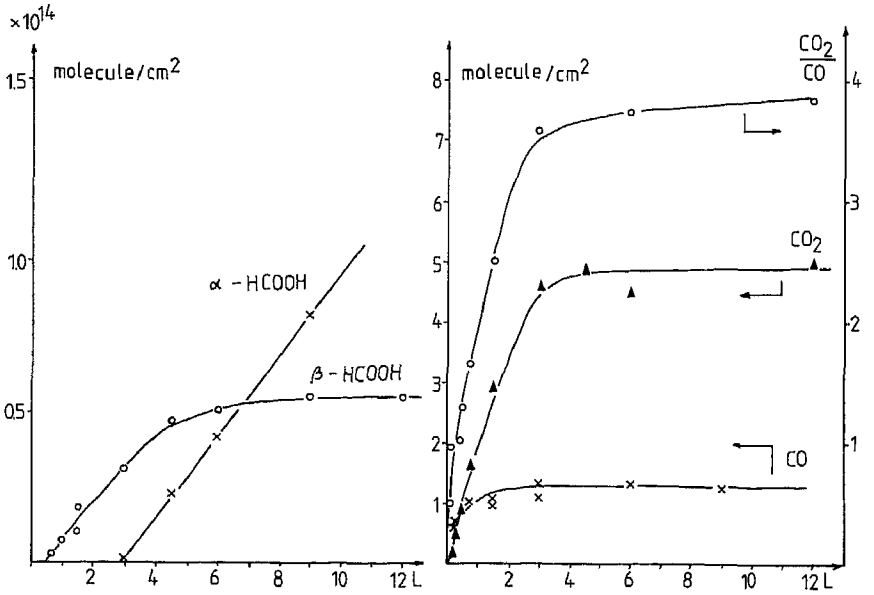

Fig. 3. The amount of desorbed products and their relations as a function of HCOOH exposure at 100 K.

When the sample was heated to higher temperatures, the intensity of the 7.9 eV loss decreased rapidly and it disappeared at around 186 K. The 11.3 and 14.8 eV losses attenuated significantly up to 160 K, but only slightly above this temperature (fig. 4). These losses were clearly detectable even at 228 K. Above this temperature, another loss feature developed at 13.1 eV from the rather broad peak. Its intensity increased up to 340 K, but then decreased. It disappeared at slightly above 500 K.

When the Rh(111) surface was exposed to HCOOH at 300 K, only one loss appeared, at 13.2 eV.

3.1.3. UPS studies

Fig. 5A shows the He II photoelectron spectra of Rh(111) as a function of the HCOOH exposure at 100 K. The adsorption of HCOOH at low exposure (0.3 L) produced an emission peak at 5.3 eV and a weak broad feature between 8 and 12 eV. At higher exposure, peaks were observed at 6.2, 8.9, 10.5, 11.9 and 16.2 eV. The positions of these peaks correspond to the formation of chemisorbed HCOOH. With the increase of the HCOOH exposure, the locations of these peaks shifted to higher energy. The shift for the low energy peak was most pronounced. At the same time, a drastic suppression in the intensity of the d-band of Rh also occurred. When the adsorbed

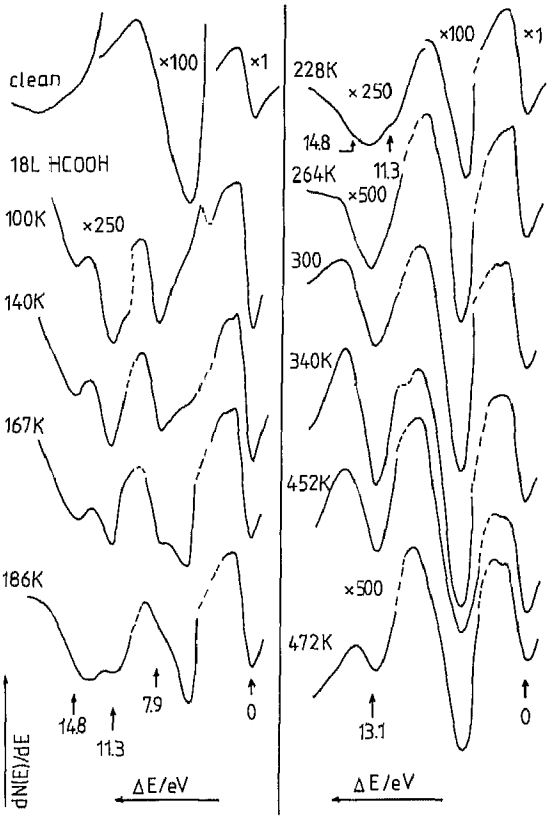

Fig. 4. Electron energy loss spectra following HCOOH adsorption on clean Rh(111) at 100 K and after gradually heating the saturated layer to different temperatures. Heating rate was 18 K s^{-1}. The heating time at a given temperature was 2 s.

layer was gradually heated to higher temperature, first the 16.2 eV peak was eliminated at 151 K, and the peak initially centred at 6.2 eV shifted to lower binding energy, to 5.3 eV (fig. 5B). A new photoemission peak at 13.2 eV,

Table 1
Binding energy data on the interaction of clean and oxygen-dosed Rh(111) with HCOOH

	T_a (K)	E_F (eV)
Clean Rh(111)	100	6.2, 8.9, 10.5, 11.9, 16.2
	151–249	5.3, 8.6, 10.2, 13.2
	267–522	8.1, 11.2
Oxygen-dosed	100	6.0, 8.1, 9.1, 10.9, 15.1
Rh(111)	215–350	5.0, 7.8, 9.2, 13.1

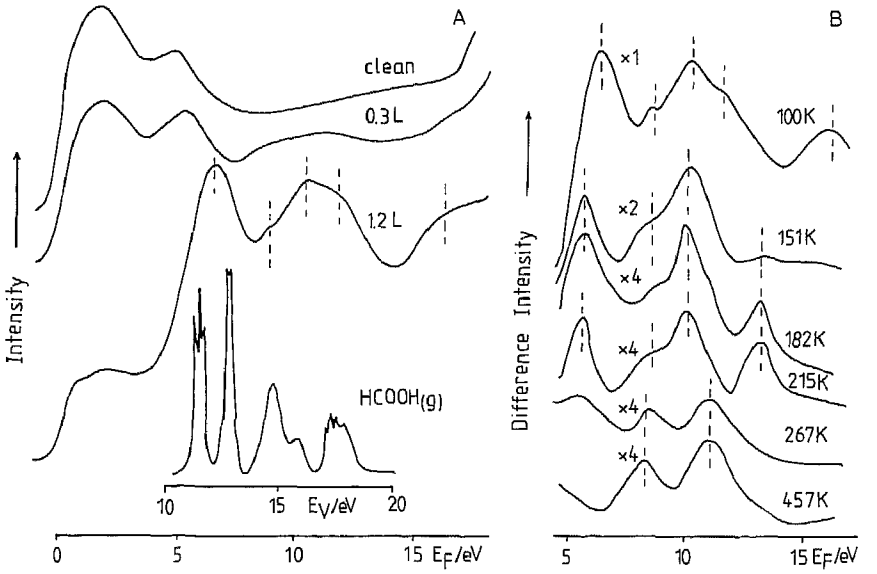

Fig. 5. He II photoelectron spectra of clean Rh(111) as a function of HCOOH exposure at 100 K (A) and after gradually heating the saturated layer to different temperatures (B). Spectrum of gaseous HCOOH is also shown [28].

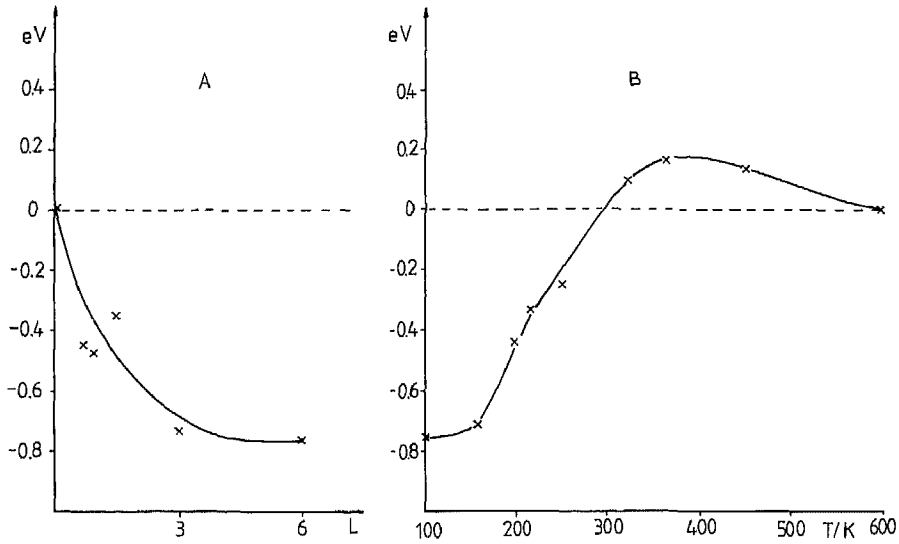

Fig. 6. Changes in the work function of clean Rh(111) as a function of HCOOH exposure at 100 K (A) and after gradually heating the saturated layer to different temperatures (B).

indicative of the formation of formate anion (see later), was also clearly detected above 151 K. All photoemission peaks, except the 13.2 eV peak, attenuated at 151–200 K. The intensity of the 13.2 eV peak started to decrease only above 215 K. This peak was completely eliminated around 249 K. Other new photoemission peaks at 8.1 and 11.2 eV (tentatively attributed to the adsorbed CO formed in the decomposition of formate species) were detectable from 267 K. Their intensity increased from 267 K up to about 286 K, and they started to attenuate above 457 K. The spectrum characteristic of clean Rh was restored at about 522 K. The observed photoemission peaks are listed in table 1.

3.1.4. Work function measurements

The exposure of a clean Rh(111) surface to HCOOH at 100 K decreased the work function of Rh by 0.75 eV at the saturation of the β-state (fig. 6). When the HCOOH-saturated (β) surface was heated, the work function gradually increased; it reached the value for a clean surface at around 300 K. It increased further up to about 360 K, but then decreased to reach the preadsorption HCOOH value by 550 K.

3.1.5. LEED studies

Finally an attempt was made to determine long-range ordered structures on Rh(111) covered with adsorbed HCOOH. The clean Rh(111) surface exhibited a sharp (1×1) pattern. Exposures of HCOOH produced no new LEED patterns at 100 K; a considerable increase in the background intensity was observed. Annealing to 170–180 K to remove the weakly bonded HCOOH did not give rise to a different picture.

3.2. Oxygen-dosed surface

3.2.1. Thermal desorption measurements

The concentration of adsorbed oxygen was calculated from the relative O Auger signal R_0 ($R_0 = h_{O_{512}}/h_{Rh_{312}}$), taking into account that at saturation the oxygen concentration is 8×10^{14} oxygen atoms/cm^2, which corresponds to $\theta_O = 0.5$ [21].

Fig. 7 shows some thermal desorption spectra as a function of oxygen coverage. Preadsorbed oxygen exerted very little influence on the desorption of condensed and chemisorbed HCOOH. The peak temperatures were hardly altered and the amounts of desorbed HCOOH in the α- and β-states differed only slightly.

A more dramatic effect was observed in the formation of the decomposition products. At $\theta_O = 0.08$ a shoulder appeared on the high-temperature side of the TD curve of CO_2 which was transformed into a new high-temperature peak. Its T_p increased from 313 K at $\theta_O = 0.08$ to 385 K at $\theta_O = 0.5$. At the

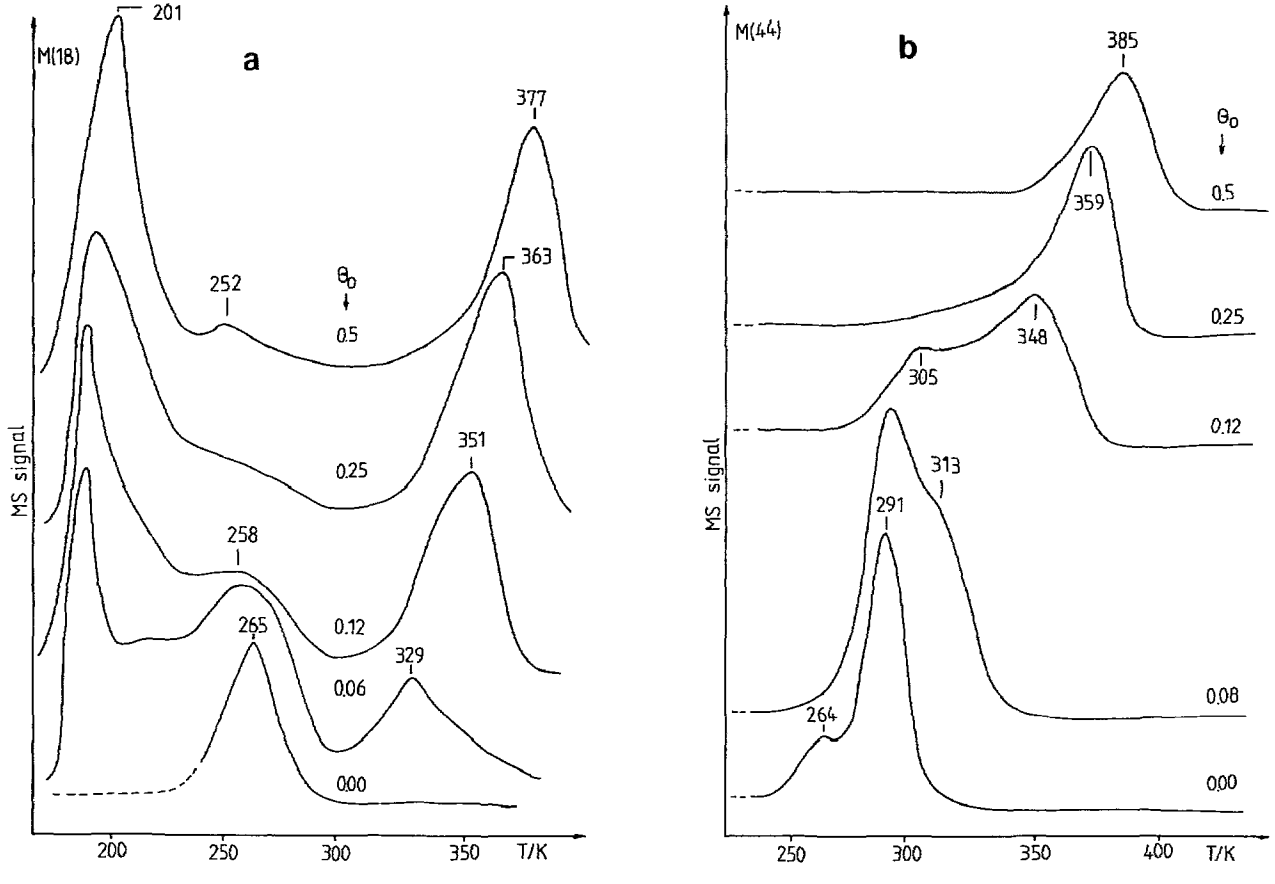

Fig. 7. Effect of oxygen coverage on the thermal desorption of H_2O (a) and CO_2 (b) following HCOOH adsorption on oxygen-dosed Rh(111) at 100 K.

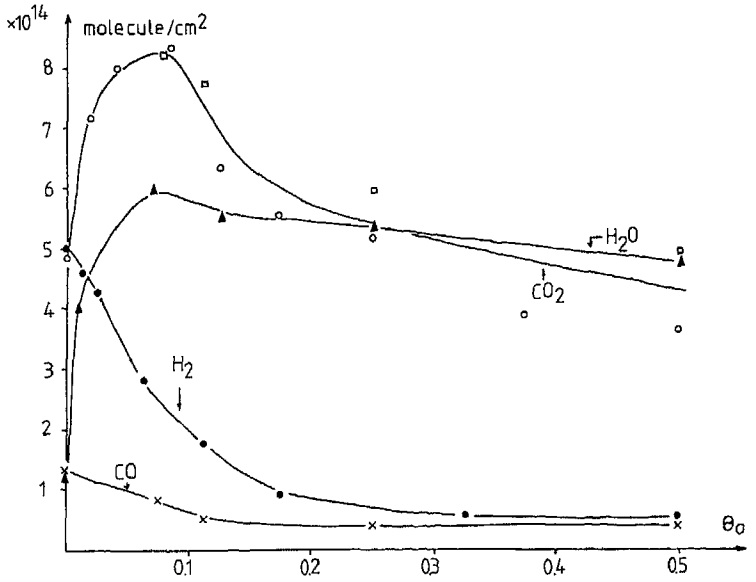

Fig. 8. Formation of H_2, CO, H_2O and CO_2 as a function of oxygen coverage on Rh(111) following HCOOH adsorption (6 L) at 100 K. Symbols, □ and ○, for CO_2 correspond to different series of experiments. The preadsorbed oxygen has been completely reacted up to about $\theta_O \approx 0.2$. At $\theta_O = 0.5$ approximately half of the preadsorbed oxygen remained on the surface.

same time, the desorption characteristic of clean Rh in the low-temperature range ceased. The amount of CO_2 produced increased up to $\theta_O = 0.08$, and then decreased. A similar feature was observed for the evolution of H_2O. The desorption at $T_p = 265$ K gradually decreased and at $\theta_O = 0.06$ new desorption peaks appeared at 184 and 329 K. These peaks became larger at higher oxygen coverage and the latter was characterized by higher T_p values. The amount of H_2 gradually decreased as the surface concentration of adsorbed oxygen increased; this was accompanied by an increase in T_p. Above $\theta_O = 0.3$, only a very small amount of H_2 (one-tenth of that determined for a clean surface) was evolved. A similar decrease was observed in the amount of CO (fig. 8).

In fig. 8, the amounts of the products formed are plotted as a function of the oxygen coverage. It shows that the sum of the amounts of CO and CO_2 exhibits a maximum at $\theta_O \approx 0.1$, which indicates that at this coverage the adsorbed oxygen increases the surface concentration of irreversibly adsorbed HCOOH, i.e. the formate species. In order to interpret these results, in a separate study we investigated the effect of preadsorbed oxygen on the desorption of H_2O and CO_2 from Rh(111). Although we found that the oxygen adatoms increase the values of T_p for both compounds, the desorption of H_2O and CO_2 occurred still at significantly lower temperatures than

following HCOOH adsorption on an oxygen dosed Rh(111) surface. This suggests that the higher temperatures for the evolution of H_2O and CO_2 in the latter case is due to the stabilization of formate species on the surface.

3.2.2. UPS studies

Fig. 9 shows the photoemission spectra of adsorbed HCOOH on oxygen covered surfaces. The preadsorbed oxygen caused a strong peak at 5.7–6.0 eV. The adsorption of HCOOH at 100 K produced the same feature as on a clean surface, but all peaks were somewhat shifted to lower binding energies (6, 8.1, 9.1, 10.9, 15.1 eV). The intensities of the peaks (at same HCOOH exposures) remained unaltered. Upon heating the adsorbed layer to higher temperature, the intensity of all photoemission peaks decreased. At 185 K a new "four-

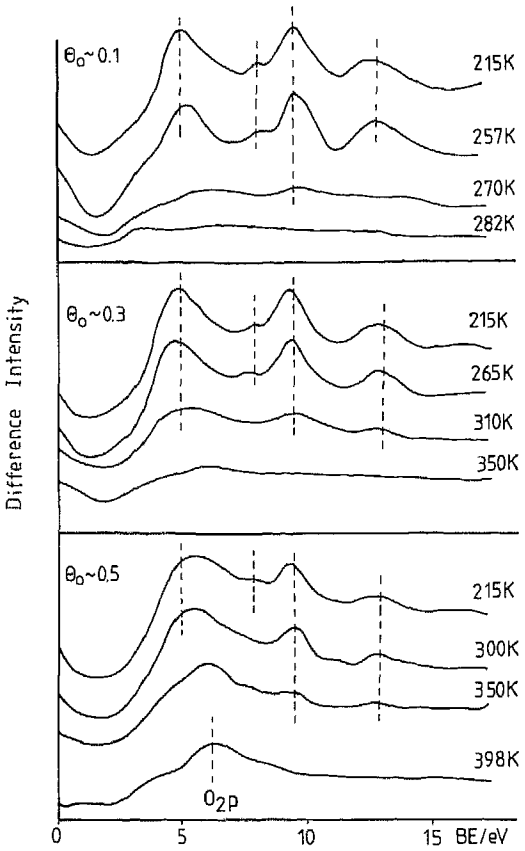

Fig. 9. He II photoelectron spectra of adsorbed HCOOH on Rh(111) at different oxygen coverages. HCOOH (2.4 L) was adsorbed at 100 K and then the sample was heated up first to 215 K to desorb the condensed HCOOH, and then to different temperatures.

peaked structure" developed, similarly to the oxygen-free surface, which was attributed to the formation of formate species. A typical feature of this spectrum is the appearance of a peak at 13.1 eV. Further raising the temperature of the sample caused an intensification of the peaks up to 215–265 K. As concerns the effect of oxygen coverage on the intensities of the peaks the optimum oxygen coverage was found to be $\theta_O = 0.1$–0.3.

Important observations are: (i) the photoemission signals on oxygen-dosed surfaces exhibited markedly higher stability than on a clean Rh and (ii) there are no other signals in the spectra due to the products of surface reactions (fig. 9). The highest temperature where the peaks were detectable showed the following variation with the oxygen coverage: 249 K at $\theta_O = 0.0$, 270 K at $\theta_O = 0.1$, 310 K at $\theta_O = 0.3$ and 350 K at $\theta_O = 0.5$.

4. Discussion

4.1. Clean surface

4.1.1. Adsorption and reactions of HCOOH

HCOOH adsorbs readily on a clean Rh(111) surface at 100 K with a high sticking probability, which decreases only slightly up to monolayer coverage. The high sticking probability, which may mean an effective energy accommodation, is characteristic of the adsorption of organic molecules which do not decompose at the adsorption temperature. The adsorption occurs in a random fashion, as LEED measurements did not reveal any long-range order after the removal of weakly adsorbed HCOOH from the surface.

The adsorption of HCOOH at 100 K produced two adsorption states. The more strongly bonded one (β) desorbed at 202 K with an activation energy of 48 kJ/mol. This state was saturated at 6 L, giving rise to an apparent surface concentration of 5.5×10^{13} HCOOH molecules/cm^2. The formation of this state caused a decrease in $\Delta\phi$. From this change it can be concluded that the species formed has a positive outward dipole moment. We suppose that the HCOOH is bonded end-on via the hydroxyl group and that the O–H bond is strongly perturbated by bonding to the surface. The weakly bonded HCOOH (α) started to develop practically immediately after the formation of the chemisorbed layer, without saturation. The desorption energy of this state is 42 kJ/mol. On the basis of the characteristics of the desorption of HCOOH in the two states, the β-peak is attributed to a monolayer, while the α-peak is ascribed to multilayers. The desorption temperature of the latter was quite similar to that of formic acid multilayers on other metals [22–25].

The fact that several other products desorbed at higher temperatures indicates that, in addition to these adsorption states, a third irreversibly adsorbed HCOOH species, very probably in the form of formate, also exists on the Rh(111) surface.

The surface concentration of irreversibly adsorbed formate (calculated from the amounts of the decomposition products CO and CO_2) is 6.3×10^{14} HCOO molecules/cm^2, while the total amount of chemisorbed HCOOH is 6.9×10^{14} HCOOH molecules/cm^2. Taking into account the surface concentration of Rh atoms on the (111) face (1.59×10^{15} atoms/cm^2), we find that the chemisorbed HCOOH occupies almost 50% of the surface Rh atoms, i.e. $\theta_{HCOOH} \approx 0.5$.

As CO_2 bonds weakly to a clean Rh(111) surface (the desorption of CO_2 following its adsorption at 100 K on Rh(111) is complete at 270 K at this coverage [26]), the evolution of CO_2 is indicative of the decomposition of the formate species on Rh(111). The data presented in fig. 2 suggest that the decomposition of formate starts at around 200 K:

$$HCOO_{(a)} \rightarrow CO_2 + H_{(a)}. \quad (1)$$

While reaction (1), the cleavage of C–H bond, is the dominant mode of decomposition of the formate species, the evolution of small amounts of H_2O and CO suggests the occurrence of the rupture of C–O bond, too:

$$HCOO_{(a)} \rightarrow H_{(a)} + CO_{(a)} + O_{(a)}, \quad (2)$$

followed by water formation in secondary reactions.

We may speculate that the structures and the bonding modes of formates decomposing according to reactions (1) and (2) are different. For convenience the first type will be denoted by A and the second type by B.

The desorption of H_2O (β) from a clean Rh(111) surface occurs above 170 K with $T_p = 182$ K [27], while in the present case T_p for H_2O evolution was 252–268 K, which is a significantly higher temperature. This feature suggests that the evolution of H_2O is a reaction-limited step. As the peak temperatures for the formation of CO agrees well with those obtained after the adsorption of CO on this surface, we conclude that the formation of CO is a desorption-limited process. The facts that both H_2O and CO formed attain their highest concentrations at low HCOOH exposure, and that the ratio CO_2/CO increases from ~ 0.5 to ~ 4 as the coverage increases indicate that the form B predominates at very low coverage, but its formation soon ceases.

Alternatively, we may assume that there are certain active sites on the Rh surface which form strong bonds with the oxygen of formate and promote the cleavage of the C–O bond. EELS measurements are planned to determine the types of formate on Rh surface and their stability region.

We may speculate as to whether the production of CO is the result of secondary reactions, namely the dissociation of CO_2. Our recent studies on the adsorption and dissociation of CO_2 over Rh clearly showed [26] that CO_2 did not dissociate on a carefully cleaned Rh(111) surface (which was actually the same sample as used in the present work). However, the dissociation of CO_2 did occur if the Rh surface contained boron impurity segregated from the bulk

[26]. It is very likely that the much larger amount of CO formed on Rh foil in the surface decomposition of HCOOH is mostly due to the effect of this boron impurity [16]. This view is supported by the EELS spectra, where an intense loss feature was produced at 9.5 eV during heating of the HCOOH-covered Rh foil to above 300 K [15].

We now have strong evidence that the 9.5 eV loss is due to some kind of boron oxide formed in a reaction between surface boron and oxygen-containing adsorbed species [27]. This loss was never produced under similar conditions on a clean Rh surface [20,26,27], and it was not detected in the present case either. We have to take also into account that the adsorbed hydrogen can promote the dissociation of CO_2 on Rh. This was observed both for supported Rh [5–10] and for Rh(111) single crystal [26]. However the extent of CO_2 dissociation on Rh(111), even under favorable condition, was much smaller than inferred from the amount of CO formed in the present case.

4.1.2. Spectroscopic features of adsorbed HCOOH

The adsorption of HCOOH has been studied by photoelectron spectroscopy on Au [28], Ni [28] and Cu [28,22] surfaces, but no UPS studies have so far been performed on the adsorption of HCOOH on Pt metals. The low-temperature photoelectron spectrum of HCOOH adsorbed on Rh(111) displays good agreement with that described previously [28]. Photoemission peaks appeared at 6.4, 8.5, 10.5, 11.9 and 16.2 eV, which are attributed to the 10a, 2b, the 9a, the 1b, the 8a, 7b and the 6a orbitals, respectively, of molecularly adsorbed HCOOH. The observed spectra are consistent with the results of gas-phase photoemission studies [28]. The difference between the spectra of the gas and condensed phases is that the two peaks due to the 10a and 2b orbitals (well separated in the gas phase at binding energies of 11.5 and 12.8 eV below the vacuum level) are not resolved in the spectrum of the condensed phase, but appear as a single broad peak at around 6.2 eV. This can be explained by the formation of HCOOH dimers [28]. Similarly as for Cu and Ni surfaces [28], the hydrogen-bonding in the dimer perturbs only the outer, 10a and 2b orbitals of the monomer.

The dissociation of HCOOH, i.e. the formation of formate, was assumed to occur on all the above metals. This was supported by well-detectable spectral changes characterized by a new four-peak structure, at 3.7–4.9, 8.1, 9.6 and 13.2 eV attributed to the $1a_2$, $6a_1$, $4b_2$, the $1b_1$, the $3b_2$, $5a_1$, and the $4a_1$ orbitals [22,28,29,30]. The UPS spectrum of adsorbed formate is in agreement with the SCF-MO molecular orbital calculations for this anion [31]. On clean Rh(111), these spectral features were clearly detected at 151 K. When our UPS spectrum is compared with those obtained for other metals or deduced from theoretical calculations, it appears that the highest-lying orbitals ($1a_2$, $6a_1$, $4b_2$) show a little perturbation due to bonding with the Rh surface. Somewhat smaller perturbations occurred in the cases of Ni [28], Cu [28] and Ag [29].

When the Rh(111) surface covered by formate was annealed at above 240 K, the peaks attributed to the formate diminished, while two new peaks were detected at 8.2 and 11.2 eV. We attribute these peaks to the $5\sigma/1\pi$ and 4σ molecular orbitals, respectively, of adsorbed CO [32,33]. These peaks were eliminated only at around 522 K, which corresponds to the desorption temperature for CO.

There was no sign of the presence of other adsorbed species, such as CO_2, which is the main product of surface decomposition. This is in accord with our finding [26] that CO_2 is weakly bonded to Rh, and desorbs at once in the temperature range 200–250 K of formate decomposition.

The EEL spectrum of adsorbed HCOOH at 100 K agreed well with those observed for Rh foil [15]. The origin of these losses has been discussed earlier in detail [15], but no comparison with UPS was made. Taking into account the energy levels of adsorbed HCOOH on the Rh(111) surface determined by UPS we assign the observed losses at 7.9, 11.3 and 14.8 eV to the intramolecular electron transitions from the 10a, 2b, the 9a, 1b, and the 8a, 7a orbitals to the unfilled 3b or 11a orbitals of HCOOH, respectively, which are situated at around 1.6–2.0 eV above the Fermi level. When the HCOOH covered Rh(111) was heated above 228 K, or HCOOH was adsorbed at 300 K, a new loss feature developed at 13.1 eV which – no doubt – belongs to the adsorbed CO formed in the surface reaction [15,20,26]. The stability regions of the losses due to chemisorbed HCOOH and CO are in accord with those deduced from TDS and UPS studies.

4.2. Oxygen-dosed surfaces

The effects of preadsorbed oxygen on the adsorption of different molecules have been investigated in great detail and well documented by Roberts and coworkers [34,35], Madix and coworkers [24,36,37] and Solymosi and coworkers [38–43].

Preadsorbed oxygen exerted a readily observable influence on the interaction of HCOOH with the Rh(111) surface:

(i) it increased the extent of dissociation of formic acid and hence the surface concentration of the formate species by a factor of 1.3 (fig. 8), and

(ii) it extended the region of stability of the surface formate by at least 80–100 K as exhibited by TDS and UPS studies (figs. 7 and 9).

The desorption of condensed and molecularly bonded HCOOH was only slightly altered by oxygen adatoms.

Qualitatively similar features were found in our laboratory for the adsorption of HNCO [38] and CH_3OH [39] on an oxygen-dosed Rh(111) surface. The promoting effect of preadsorbed oxygen in the dissociation of HCOOH can be attributed to the reaction

$$O_{(a)} + HCOOH_{(g)} \rightarrow OH_{(a)} + HCOO_{(a)}, \qquad (3)$$

i.e. to the formation of a strong O–H bond. In other words the oxygen adatom reacts as a Brönsted base toward HCOOH, by abstracting the acidic hydrogen from HCOOH [24]. The resulting adsorbed OH groups interact and H_2O is desorbed:

$$OH_{(a)} + OH_{(a)} \rightarrow O_{(a)} + H_2O_{(g)}, \quad (4)$$

with $T_p = 215$ K [44]. Although careful analysis of the TD curves for H_2O reveals desorption at this temperature, a larger amount of H_2O is desorbed at 184–200 K. This suggests that, in addition to steps 3 and 4, it is also necessary to consider the occurrence of the reaction

$$OH_{(a)} + HCOOH \rightarrow HCOO_{(a)} + H_2O_{(g)}. \quad (5)$$

An interesting feature of the effect of preadsorbed oxygen is the significant stabilization of formate on Rh. The fact that the proton reacts with adsorbed oxygen (and is desorbed in the form of H_2O) can certainly contribute to the increases in the lifetime and stability of adsorbed formate, as it lowers the probability of the reverse reaction, i.e. the associative desorption of the molecule. Another factor which should be taken into account is the blocking of the Rh sites required for the decomposition of the formate species and for the binding of CO and H. This could be important when the binding of the decomposition products requires a larger number of surface sites than the number occupied by the adsorbed molecule before decomposition, and when the products form strong bonds with the metals (e.g. in NCO and CH_3O decompositions), but this is less significant in the present case.

For the NCO + O/Rh(111) system we proposed that the stabilizing effect of preadsorbed oxygen occurs through a ligand effect, which results in a more ionic bond, and thereby in a higher stability [38]. A shift in the ν_{as}(NCO) loss towards higher frequency [38,40] strongly supported this view. We believe that this ligand effect plays an important role in the enhanced stability of the formate species on oxygen-dosed Rh surfaces, too.

An alternative mode of stabilization of the formate species would be a structural rearrangement, i.e. an oxygen-induced transformation of the formate into a more stable form.

In the presence of adsorbed oxygen we experienced a significant change in the product distribution; the amounts of CO_2 and particularly H_2O increased greatly at the expense of H_2 and CO, indicating that an oxidation process too occurred on the surface:

$$CO_{(a)} + O_{(a)} \rightarrow CO_{2(g)} \quad (6)$$

and/or

$$2\,HCOO_{(a)} + O_{(a)} \rightarrow 2CO_2 + H_2O. \quad (7)$$

One could also consider a variation in the selectivity of formate decomposition as a function of oxygen coverage. The fact that the values of T_p for the new peaks of CO_2 and H_2O (caused by preadsorbed oxygen) are practically identical at the same oxygen coverages (T_p = 329–377 K) strongly supports the idea that they are formed in the same surface reaction, very likely in the direct oxidation of formate species. This reaction was also assumed to occur on an Au(110) surface [24].

5. Catalytic implications

As outlined in the introduction, formate is considered to be an important surface intermediate in several catalytic reactions on Rh catalyst. The results of the present study demonstrate that formate is an unstable species on a clean Rh surface: it decomposes completely at around 300 K. However, chemisorbed oxygen greatly enhances the stability of formate on Rh. Hence, it seems quite possible that, due to this stabilizing effect, the formate species has a sufficient lifetime on supported Rh, even at higher temperature, to function as a surface intermediate in the catalytic synthesis of oxygenated compounds in the hydrogenation of carbon oxides.

References

[1] D.C. Grenoble, M.M. Estadt and D.F. Ollis, J. Catalysis 67 (1981) 90.
[2] A. Kienemann, J.P. Hindermann, R. Brault and H. Idriss, Am. Chem. Soc. Div. Petrol. Chem. 31 (1986) 46.
[3] F. Solymosi, I. Tombácz and M. Kocsis, J. Catalysis 75 (1982) 78.
[4] M. Ichikawa and K. Shikakura, in: Proc. 7th Intern. Congr. on Catalysis, Tokyo, 1980, Part B, p. 925.
[5] F. Solymosi, A. Erdöhelyi and T. Bánsági, J. Catalysis 68 (1981) 371.
[6] M.A. Henderson and S.D. Woorley, J. Phys. Chem. 89 (1985) 1417.
[7] T. Iizuka, Y. Tanaka and K. Tanabe, J. Mol. Catalysis 17 (1982) 381.
[8] F. Solymosi, A. Erdöhelyi and T. Bánsági, J. Chem. Soc. Faraday Trans. I, 77 (1981) 2645.
[9] F. Solymosi, A. Erdöhelyi and M. Kocsis, J. Catalysis 65 (1980) 428.
[10] Y. Tanaka, T. Iizuka and K. Tanabe, J. Chem. Soc. Faraday Trans. I, 78 (1982) 2215.
[11] F. Solymosi, T. Bánsági and A. Erdöhelyi, J. Catalysis 72 (1981) 166.
[12] A. Deluzarche, J.P. Hindermann, R. Kieffer, J. Cressely, R. Stupler and A. Kienemann, Spectra 2000, 75 (1982) 27.
[13] A. Deluzarche, J.P. Hindermann, A. Kienemann and R. Kieffer, J. Mol. Catalysis 31 (1985) 295.
[14] A. Deluzarche, J.P. Hindermann, R. Kieffer and A. Kienemann, Rev. Chem. Intermed. 6 (1985) 625.
[15] F. Solymosi and J. Kiss, J. Catalysis 81 (1983) 95.
[16] F. Solymosi, J. Kiss and I. Kovács, J. Phys. Chem., in press.
[17] S. Anderson and U. Jostell, Surface Sci. 46 (1974) 625.
[18] K. Christmann and J.E. Demuth, J. Chem. Phys. 76 (1982) 6318.

[19] J. Kiss and F. Solymosi, Surface Sci. 135 (1983) 243.
[20] F. Solymosi, A. Berkó and T.I. Tarnóczi, Surface Sci. 141 (1984) 533.
[21] P.A. Thiel, J.T. Yates, Jr. and W.H. Weinberg, Surface Sci. 82 (1979) 72.
[22] M. Bowker and R.J. Madix, Surface Sci. 102 (1981) 542.
[23] B.A. Sexton and R.J. Madix, Surface Sci. 105 (1981) 177.
[24] D.A. Outka and R.J. Madix, Surface Sci. 179 (1987) 361.
[25] N.R. Avery, Appl. Surface Sci. 11/12 (1982) 774.
[26] F. Solymosi and J. Kiss, Surface Sci. 149 (1985) 17.
[27] J. Kiss and F. Solymosi, Surface Sci. 177 (1986) 191.
[28] R.W. Joyner and M.W. Roberts, Proc. Roy. Soc. (London) A350 (1976) 107.
[29] M.A. Barteau and R.J. Madix, Surface Sci. 120 (1982) 262.
[30] B.A. Sexton, A.E. Hughes and N.R. Avery, Surface Sci. 155 (1985) 366.
[31] S.D. Peyerimhoff, J. Chem. Phys. 47 (1967) 349.
[32] C.L. Allyn, T. Gustafsson and W.W. Plummer, Chem. Phys. Letters 47 (1977) 127.
[33] D.E. Peebles, H.C. Peebles and J.W. White, Surface Sci. 136 (1984) 463.
[34] M.W. Roberts, Advan. Catalysis 29 (1980) 55.
[35] S.A. Isa, R.W. Joyner, M.H. Matloob and M.W. Roberts, Appl. Surface Sci. 5 (1980) 345.
[36] R.J. Madix, Advan. Catalysis 29 (1980) 1.
[37] M.A. Barteau, M. Bowker and R.J. Madix, Surface Sci. 94 (1980) 303.
[38] F. Solymosi, A. Berkó and T.I. Tarnóczi, Appl. Surface Sci. 18 (1984) 233.
[39] F. Solymosi, T.I. Tarnóczi and A. Berkó, J. Phys. Chem. 88 (1984) 6170.
[40] M. Surman, S.R. Bare, P. Hofmann, F. Solymosi and D.A. King, to be published.
[41] F. Solymosi and J. Kiss, Surface Sci. 104 (1981) 181.
[42] F. Solymosi and A. Berkó, Surface Sci. 122 (1982) 275.
[43] F. Solymosi and L. Bugyi, Surface Sci. 147 (1984) 685.
[44] J.J. Zinck and W.H. Weinberg, J. Vacuum Sci. Technol. 17 (1980) 188.